

Accepted Manuscript

Synthesis of loofah sponge carbon supported bimetallic silver-cobalt nanoparticles with enhanced catalytic activity towards hydrogen generation from sodium borohydride hydrolysis

Lunhong Ai, Xiaomin Liu, Jing Jiang

PII: S0925-8388(14)02783-2

DOI: <http://dx.doi.org/10.1016/j.jallcom.2014.11.135>

Reference: JALCOM 32689

To appear in: *Journal of Alloys and Compounds*

Received Date: 15 September 2014

Revised Date: 30 October 2014

Accepted Date: 21 November 2014

Please cite this article as: L. Ai, X. Liu, J. Jiang, Synthesis of loofah sponge carbon supported bimetallic silver-cobalt nanoparticles with enhanced catalytic activity towards hydrogen generation from sodium borohydride hydrolysis, *Journal of Alloys and Compounds* (2014), doi: <http://dx.doi.org/10.1016/j.jallcom.2014.11.135>

This is a PDF file of an unedited manuscript that has been accepted for publication. As a service to our customers we are providing this early version of the manuscript. The manuscript will undergo copyediting, typesetting, and review of the resulting proof before it is published in its final form. Please note that during the production process errors may be discovered which could affect the content, and all legal disclaimers that apply to the journal pertain.



**Synthesis of loofah sponge carbon supported bimetallic
silver-cobalt nanoparticles with enhanced catalytic activity
towards hydrogen generation from sodium borohydride
hydrolysis**

Lunhong Ai, Xiaomin Liu, Jing Jiang*

*Chemical Synthesis and Pollution Control Key Laboratory of Sichuan Province, College of
Chemistry and Chemical Engineering, China West Normal University, Nanchong 637002, P.R.
China*

Abstract

We demonstrate a functionalized carbonaceous material derived from the hydrothermal carbonization of natural loofah sponge can be served as an effective scaffold for anchoring bimetallic AgCo nanoparticles (NPs). The resulting loofah sponge carbon (LSC) supported AgCo NPs (LSC/AgCo) exhibits excellent performance for the catalytic hydrolysis of NaBH₄ towards hydrogen generation. It is experimentally proved that the existed AgCo NPs mainly contribute to the catalytic activity, while the employed LSC support make them more effective in LSC/AgCo catalytic systems. The catalytic activities of the LSC/AgCo catalysts are also strongly dependent on the Ag/Co ratio, where LSC/Ag_{0.1}Co_{0.9} is most active among all of the catalysts, and even more than five times that of monometallic LSC/Co, revealing that the Ag and Co compositions in LSC/AgCo catalysts show excellent synergy to catalyze NaBH₄ hydrolysis for hydrogen generation. The present experimental study provides a promising pathway for the economical

* Corresponding author. Tel./Fax: +86 817 2568081.

E-mail address: 0826zjjh@163.com (J. Jiang)

and sustainable implementation of biomass for the chemical hydrogen storage.

Keywords: Nanoparticles; Catalyst; Hydrogen generation; Sodium borohydride; Hydrolysis

1. Introduction

The extensive utilization of traditional fossil fuels causes severe environmental problem and energy crisis. This major concern drives the increased demand for the exploration of the new clean energy sources to meet the sustainability of human society [1, 2]. Hydrogen appears to be one of most ideal and cleanest energy sources, which is considered to be a promising candidate for a leading energy source in the future, due to its high gravimetric energy density, ideal combustion efficiency and non-toxicity. However, the efficient and safe hydrogen storage is still a critical issue for the practical implementation. Sodium borohydride (NaBH_4) with high gravimetric density (10.8 wt%) and volumetric hydrogen density ($113 \text{ kg}\cdot\text{m}^{-3}$) has been regarded as an attractive candidate for hydrogen storage [3, 4], which can supply pure hydrogen by room-temperature hydrolysis reaction ($\text{NaBH}_4 + 2\text{H}_2\text{O} \rightarrow \text{NaBO}_2 + 4\text{H}_2 \uparrow$). However, a favourable catalyst is required to accelerate this hydrolysis reaction in a controllable manner for practical applications. Among a wide variety of available catalysts, noble metals such as Pt and Pt-based alloys show unbeatable catalytic activity. However, the high cost and low abundance of noble metals and alloys restrict their widespread application. Therefore, it is of great interest to design and fabricate cost-effective alternatives to precious and low abundant Pt catalyst to gain a sustainable hydrogen production from the NaBH_4 hydrolysis reaction.

Cobalt is much more abundant than precious metals, which has emerged as an interesting non-noble metal for its catalytic ability toward hydrogen generation. Particularly, it has been recently reported that Co-based bimetallic systems are catalytically active toward the NaBH_4

hydrolysis for hydrogen generation, due to the combined properties of the two individual metals derived from the electronic effects and geometric effects [5-7]. For example, CoPd bimetallic nanoparticles (BNPs) obtained by a unique solution phase synthesis showed the composition-dependent activity for the hydrolysis and methanolysis of ammonia borane at room temperature [8, 9]. The $\text{Co}_{35}\text{Pd}_{65}$ and $\text{Co}_{48}\text{Pd}_{52}$ BNPs were the most active catalyst in the hydrolysis and methanolysis of ammonia borane, respectively. Other Co-based alloy catalysts such as M@Co (M = Au [10] and Cu [11]) explored by Xu's group also showed a significantly higher catalytic activity than their monometallic counterparts. In addition, to further enhance the catalytic activity, the robust support should be introduced to protect BNPs against dissolution and aggregation. Cheng et al. systematically investigate a number of graphene-supported BNPs catalysts and found that these supported catalytic systems exhibited the enhanced hydrogen generation rates with respect to free BNPs [12-15]. Xu et al. have developed several remarkable BNPs catalysts by anchoring them on the porous metal-organic frameworks (MOFs), and observed the interesting synergistic catalysis phenomenon [16-19]. Therefore, combining the designable BNPs and the effective support to the obtainable synergistic catalysis should be a desirable strategy to achieve the enhanced catalytic efficiency and dramatically lower the application cost.

Inspired our recent study on the cost-effective biomass-derived catalysts [20-22], we herein report the economical and efficient bimetallic catalytic systems that can be fabricated by a carbonaceous material derived from the hydrothermal carbonization of natural loofah sponge. The loofah sponge carbon (LSC) supported AgCo NPs (LSC/AgCo) show superior performance for catalyzing hydrolysis of NaBH_4 toward hydrogen generation. Combining with Ag

significantly enhances the catalytic activity of Co and the catalytic activity of LSC/AgCo can be improved by controlling their compositions, where the optimum activity is observed for LSC/Ag_{0.1}Co_{0.9}. By taking advantage of structural properties, the LSC/Ag_{0.1}Co_{0.9} also exhibits more remarkable activity than that of free Ag_{0.1}Co_{0.9} NPs. The present experimental study provides an effective pathway for the economical and sustainable implementation of biomass for the chemical hydrogen storage.

2. Experimental

2.1. Materials

Co(NO₃)₂·6H₂O, AgNO₃, NaBH₄, and NaOH were purchased from Kelong Chemical Reagents Company (Chengdu, China) and used without further purification. All chemicals used in this study were of commercially available analytical grade.

2.2. Hydrothermal synthesis of LSC

The loofah sponges were directly obtained from a local farm (Huafeng town, Nanchong City, China). The carbonaceous sponges were prepared by a hydrothermal carbonization method using loofah sponges as the carbon source. The loofah sponge was cut into different sizes and put into a Teflon-lined stainless-steel autoclave and hydrothermally treated at 180 °C for 18 h. After that, the loofah sponge carbon (LSC) was collected, washed with distilled water several times, and dried in vacuum at 60 °C for 24 h.

2.3. Fabrication of LSC/AgCo catalysts

AgCo BNPs supported on LSC were fabricated by the chemical reduction during the catalytic hydrolysis of NaBH₄. In a typical experiment of LSC/Ag_{0.1}Co_{0.9}, 0.01 g LSC, 0.18 mmol Co(NO₃)₂·6H₂O and 0.02 mmol AgNO₃ were added in 4.5 mL deionized water kept in a flask.

After ultrasonication for about 15 min, 4.5 mL alkaline solution containing 0.5 g NaBH_4 and 0.5 g NaOH were rapidly added into flask. AgCo BNPs were formed on LSC and the catalytic hydrolysis of NaBH_4 started immediately. To find the composition-dependent activity, LSC/ $\text{Ag}_x\text{Co}_{1-x}$ ($x = 0, 0.1, 0.2, 0.3, 0.5, \text{ and } 1$) catalysts with various Ag/Co ratios were synthesized by varying the concentration of Ag and Co salts in initial solution, where x represents the molar portion of silver and the total molar amount of (Ag + Co) was kept at a constant of 0.2 mmol.

2.4. Characterization

The X-ray diffraction (XRD) measurements were recorded on a Rigaku Dmax/Ultima IV diffractometer with monochromatized Cu $K\alpha$ radiation ($\lambda = 0.15418 \text{ nm}$). The morphology was observed with a JEOL 6700-F scanning electron microscope (SEM) and transmission electron microscope (TEM, FEI Tecnai G20). The elemental composition of the samples were characterized by energy-dispersive X-ray spectroscopy (EDX, Oxford instruments X-Max). Surface electronic states were analyzed by X-ray photoelectron spectroscopy (XPS, Perkin-Elmer PHI 5000C, Al KR). All binding energies were calibrated by using the contaminant carbon ($\text{C}_{1s} = 284.6 \text{ eV}$) as a reference. The Fourier transform infrared (FTIR) spectroscopy was recorded on Nicolet 6700 FTIR Spectrometric Analyzer using KBr pellets.

2.5. Hydrogen generation measurement

The hydrogen generation experiments were performed by a classic water-displacement method. An alkaline-stabilized solution of NaBH_4 (9 mL, 5 wt%) was prepared by the addition of NaOH (5 wt%) in a flask for catalytic activity tests. The flask was immersed in thermostatic water bath to maintain at a given temperature. During the catalytic process, no stirring was adopted due to

the presence of vigorous bubble induced by the generated hydrogen, facilitating the contact between the reactant and the catalyst. For each test, the amount of LSC support was kept the same (0.01 g) and the total molar amount of (Ag + Co) was kept at a constant of 0.2 mmol. Different experimental parameters such as NaOH concentrations, NaBH₄ concentrations, and temperature were varied for the detailed study on NaBH₄ hydrolysis catalyzed by the LSC/AgCo. The activation energy was determined by test of hydrogen generation rates at different temperatures. For recyclability tests, the hydrolysis reactions were repeated four times. The first run refers to the in situ reduction and simultaneous NaBH₄ hydrolysis reaction. For the second to fourth run, the experiments were carried out in an equivalent volume (9 mL) of 5 wt% NaBH₄ solution containing 5 wt% NaOH.

3. Results and discussion

Loofah sponges are widely used in the kitchen washing in Chinese family, which can be easily obtained from the fully ripened loofah plant by removal of the skins and seeds. As shown in Fig. 1, the natural loofah sponge is consisted of the continuous, flexible, interconnected junction-like three-dimensional (3D) structure, offering mechanically stable scaffold. Additionally, the abundant oxygen-containing functional groups, such as hydroxyl group (3429 cm⁻¹), C=O bond (1633 cm⁻¹), O-C=O bond (1633 cm⁻¹ and 1450 cm⁻¹) and O-C-O bond (1503.6 cm⁻¹), on the structure of LSC (Fig. 2), provide the relatively active surface sites for the immobilization of metallic NPs. Fig. 1 schematically illustrates the fabrication strategy of LSC/AgCo catalysts. The LSC can be directly obtained by the hydrothermal treatment of the natural loofah sponges. The Ag⁺ and Co²⁺ ions would be easily enriched around the LSC due to the interaction between negative oxygen-containing groups and metallic cations. The black LSC/AgCo catalysts were

finally produced by addition of NaBH_4 during chemical reduction process.

The phase structure and crystallinity of the synthesized samples were characterized by X-ray diffraction (XRD). Fig. 3 shows the typical XRD patterns of the LSC, free $\text{Ag}_{0.1}\text{Co}_{0.9}$ and $\text{LSC}/\text{Ag}_{0.1}\text{Co}_{0.9}$. The bare LSC shows a broad peak centered at $2\theta = 22.6^\circ$, corresponding to the amorphous carbon. For the free $\text{Ag}_{0.1}\text{Co}_{0.9}$, three diffraction peaks at $2\theta = 38.0^\circ$, 44.2° and 64.5° can be well matched with the standard XRD pattern of metallic Ag (JCPDS file no. 04-0783). Notably, no detectable peaks assigned to metallic Co was observed in the pattern, indicating the amorphous nature of Co component. This phenomenon was very similar to the previous observations for Co-based bimetallic system [13-15]. The relatively high crystallinity of metallic Ag in bimetallic $\text{Ag}_{0.1}\text{Co}_{0.9}$ could be attributed to the higher reduction potentials of Ag^+/Ag^0 (reduction potentials: $E^0_{\text{Ag}^+/\text{Ag}^0} = 0.7996 \text{ eV vs. SHE}$; $E^0_{\text{Co}^{2+}/\text{Co}^0} = 0.28 \text{ eV vs. SHE}$). Thus, Ag^+ can be firstly reduced to metallic Ag prior to Co^{2+} , which is beneficial for the subsequent crystal nucleation and growth. In the case of $\text{LSC}/\text{Ag}_{0.1}\text{Co}_{0.9}$, except the typical diffraction peaks of $\text{Ag}_{0.1}\text{Co}_{0.9}$, a new broad peak corresponding to the LSC located at $2\theta = 22.6^\circ$ can be found, confirming the coexistence of $\text{Ag}_{0.1}\text{Co}_{0.9}$ and LSC in the product.

The morphologies and microstructures of the LSC, free $\text{Ag}_{0.1}\text{Co}_{0.9}$ and $\text{LSC}/\text{Ag}_{0.1}\text{Co}_{0.9}$ were observed by scanning electron microscopy (SEM). As shown in Fig. 4a, the individual LSC with a diameter of 300 μm looks like a tree stump with several shallow channels and small fractures. The magnified SEM image (Fig. 4b) reveals that the slightly rough surface of the LSC is wrinkled due to the shrinkage of plant tissues in the loofah sponge during the hydrothermal treatment process. This unique structure of LSC should be beneficial to the loading of metallic NPs. Fig. 4c and Fig. 4d show the typical SEM images of free $\text{Ag}_{0.1}\text{Co}_{0.9}$, which are composed of

spherical particles with size distribution within 50-100 nm. It is clear that these $\text{Ag}_{0.1}\text{Co}_{0.9}$ NPs suffer from serious aggregation due to their high surface energy and magnetic interaction. As shown in Fig. 4e, the $\text{Ag}_{0.1}\text{Co}_{0.9}$ can be grown and stabilized on the LSC support. Unlike the bare LSC, the surface of the LSC seems to be not smooth, where the fine $\text{Ag}_{0.1}\text{Co}_{0.9}$ NPs are anchored on firmly. Different from free $\text{Ag}_{0.1}\text{Co}_{0.9}$ (Fig. 4c), the fine $\text{Ag}_{0.1}\text{Co}_{0.9}$ NPs achieve good dispersion in the presence of the LSC (Fig. 4f), which is critical to heterogeneous catalysis applications. The microstructure of $\text{LSC}/\text{Ag}_{0.1}\text{Co}_{0.9}$ was further characterized by transmission electron microscopy (TEM). As shown in Fig. S1a, the $\text{Ag}_{0.1}\text{Co}_{0.9}$ NPs are well-loaded on the LSC matrix. No free NPs are found outside of the LSC support during the TEM observation, indicating a perfect combination between the LSC and $\text{Ag}_{0.1}\text{Co}_{0.9}$ NPs. The high-magnified TEM image (Fig. S1b, Supporting Information) further shows that the crystalline Ag (dark region) is fully surrounded by the amorphous Co (grey region), suggesting that Ag is initially reduced by NaBH_4 , and acts as the center helping for the subsequent growth of Co. Such structure of Ag surrounded by Co is consistent with the previous observations on bimetallic AgCo systems [15, 23, 24]. Moreover, the d-spacing of the crystallized dark region (inset in Fig. S1b, Supporting Information) is 0.236 nm, corresponding to the Ag(111) plane spacing.

The elemental composition and electronic structure of the $\text{LSC}/\text{Ag}_{0.1}\text{Co}_{0.9}$ were determined by X-ray photoelectron spectroscopy (XPS). Fig. 5a shows high-resolution XPS spectrum of the C1s. Three surface components in the spectrum at approximately 284.8 eV (C-C or C-H), 286.3 eV (C-OH or C-O) and 289.0 eV (O-C=O) [25, 26]. The high-resolution XPS spectrum of the O 1s (Fig. 5b) is fitted by four chemical states at binding energies of 531.2, 532.1, 535.9 and 530.6 eV, which can be ascribed to O in the form of C=O, C-O, B-O, O-H from adsorbed water [25, 26]

and Co-O bond due to oxidation of metallic Co [27], respectively. As shown in Fig. 5c, the binding energies at 778.5 and 781.2 eV correspond to metallic Co(0) and surface Co(II) species due to the partial surface oxidization, respectively. The shakeup satellite peak (786.2 eV) at approximately 5 eV above the main peak is further evidence of surface Co(II) species. The detectable Co(II) species can be ascribed to the surface Co combined with oxygen of atmosphere during the catalyst preparation and storage process, which is similar to the other cobalt-based catalysts [13-15]. The Ag 3d core level spectrum (Fig. 5d) shows two distinct peaks at 367.7 and 373.7 eV, which could be attributed to Ag 3d_{5/2} and Ag 3d_{3/2} of metallic Ag, respectively. Meanwhile, the 6.0 eV difference between the binding energies of Ag 3d_{5/2} and Ag 3d_{3/2} is also characteristic of the metallic Ag 3d states [28], confirming the presence of air-stable metallic Ag in the LSC/AgCo product. Of note, a prominent peak at around 192 eV assigned to B-O in BO₂⁻ species appears in the high-resolution XPS spectrum of the B 1s (Fig. S2, Supporting Information), suggesting that a certain amount of NaBO₂ by-product may be deposited on the sample surface during preparation process [29]. In addition, the energy-dispersive X-ray spectrometry (EDX) also confirms these elements coexisted in the LSC/Ag_{0.1}Co_{0.9} (Fig. S3, Supporting Information). The composition of Ag:Co ratio in the LSC/Ag_{0.1}Co_{0.9} is found to be approximately 89.75:10.25, which is very close to its feeding ratio.

The catalytic activities of LSC/AgCo were evaluated by the hydrolysis of NaBH₄ for hydrogen generation. Fig. 6 shows the amounts of generated hydrogen from NaBH₄ aqueous solution as a function of reaction time by using various catalytic systems. The LSC as a catalyst is incapable of catalyzing the hydrolysis of NaBH₄, evidenced by the negligible hydrogen generation. In contrast, the considerable hydrogen generation occurred under same reaction condition in the

presence of free AgCo NPs ($\text{Ag}_{0.1}\text{Co}_{0.9}$), indicating the AgCo NPs are active in the catalytic hydrolysis of NaBH_4 . Interestingly, after combination with the LSC support, the obtained LSC/ $\text{Ag}_{0.1}\text{Co}_{0.9}$ exhibits more remarkable catalytic activity toward NaBH_4 hydrolysis than that of free $\text{Ag}_{0.1}\text{Co}_{0.9}$, where the corresponding reaction rate constant increases from $65.84 \text{ mL}\cdot\text{min}^{-1}$ to $82.01 \text{ mL}\cdot\text{min}^{-1}$. We thereby deduce that the catalytic ability should be originated from the existed $\text{Ag}_{0.1}\text{Co}_{0.9}$ component, whereas enhanced efficiency could be attributed to the cooperation between LSC and $\text{Ag}_{0.1}\text{Co}_{0.9}$. Furthermore, the LSC/AgCo presents the composition-dependent catalytic activity, as shown in Fig. 7a. No detectable hydrogen generation is observed for LSC/Ag, while the moderate amounts of hydrogen generation was produced by LSC/Co. Interestingly, the bimetallic LSC/AgCo exhibits much higher catalytic activity than that of monometallic LSC/Ag and LSC/Co, appearing the accelerated hydrogen generation performance. However, the activity differences among them could be still clearly distinguished. The rationally controlled Ag content in LSC/AgCo is critical to the optimized catalytic activity. The apparent reaction rate constants were calculated to be 82.01, 58.92, 37.2 and $38.99 \text{ mL}\cdot\text{min}^{-1}$ for LSC/ $\text{Ag}_{0.1}\text{Co}_{0.9}$, LSC/ $\text{Ag}_{0.2}\text{Co}_{0.8}$, LSC/ $\text{Ag}_{0.3}\text{Co}_{0.7}$, and LSC/ $\text{Ag}_{0.5}\text{Co}_{0.5}$, respectively. The LSC/ $\text{Ag}_{0.1}\text{Co}_{0.9}$ achieves the best catalytic activity toward the hydrolysis of NaBH_4 among all of the samples. The qualitative analysis further reveals that LSC/ $\text{Ag}_{0.1}\text{Co}_{0.9}$ possesses a catalytic activity of 3.07 times that of Ag-absent LSC/Co (Fig. 7b). Considering the poor catalytic performance of individual components, a synergetic interaction between Ag and Co in LSC/AgCo plays a critical role in catalytic reaction. As widely accepted, bimetallic system is a well-known phenomenon that can remarkably improve the catalytic activity of the original monometal catalysts for different chemical processes [30-32]. In our case, the excellent catalytic

activity of LSC/Ag_{0.1}Co_{0.9} is attributed to the combination of strain and ligand effects caused by the atomic environment of distinct metal atoms on bimetallic surfaces, which could be promoted by the surface plasmon resonance (SPR) effect of metallic Ag NPs [33]. The SPR-induced oscillating electric fields would deepen the d-band center position of the neighbouring Co atoms, leading to their low adsorption energy and high reactivity [34]. Based on these considerations, it is reasonable to believe that the supporting effect of LSC and intermetallic electronic interactions between Ag and Co in LSC/AgCo catalysts could cooperate together to catalyze NaBH₄ hydrolysis to significantly promote the hydrogen generation.

Fig. 8 shows the effect of variation in NaOH concentrations on hydrogen generation performance over LSC/Ag_{0.1}Co_{0.9}. Although the addition of NaOH could efficiently inhibit the self-hydrolysis of NaBH₄, the catalytic activity of LSC/Ag_{0.1}Co_{0.9} is still closely dependent on the NaOH concentration. For example, when the NaOH concentrations were increased in the range of 1-5 wt%, the hydrogen generation rates were accelerated markedly from 43.44 to 82.01 mL·min⁻¹. However, further increasing the NaOH concentrations up to 10 wt% leads to significantly lowering the rate of hydrogen generation. This phenomenon is very similar to the previous observations reported in other catalytic systems [35-37]. In terms of these results, it is expected that NaOH plays multiple roles for the catalytic hydrolysis of NaBH₄. An appropriate amount of NaOH is critical to the catalytic activity, ensuring stability of NaBH₄ in aqueous solution, while the excess amounts of added NaOH increase the alkalinity and viscosity of the solution, retarding the mass transfer rate in catalytic systems.

Fig. 9 shows the effect of NaBH₄ concentrations on the catalytic activity of LSC/Ag_{0.1}Co_{0.9}. As a hydrogen source in the hydrolysis reaction, kinetics of the catalytic reaction should be

associated with NaBH_4 concentration. It is clear that hydrogen generation rate increases remarkably with increasing NaBH_4 concentration from 1 wt% to 5 wt%, and then keeps almost a constant when further increasing NaBH_4 concentration to 10 wt%. However, hydrogen generation rate was found to decline as the NaBH_4 concentration reaches up to 15 wt%. This is mainly ascribed to following two aspects: (1) increasing NaBH_4 concentration results in the increased viscosity of reaction medium, slowing down the mass transfer rate; (2) the self-formed NaBO_2 with relatively lower solubility could destroy active sites on the catalyst surface and interrupt contact between catalyst and NaBH_4 . Thereby, these results clearly indicate that in order to achieve high hydrogen generation rates, both NaBH_4 and NaOH should be controlled in the appropriate concentrations.

Fig. 10a shows the catalytic activity of $\text{LSC/Ag}_{0.1}\text{Co}_{0.9}$ toward the hydrolysis of NaBH_4 at different temperatures. It can be clearly seen that this catalytic reaction is very sensitive to this parameter. More specifically, when the temperature was increased from 20 to 50 °C, the rates of hydrogen generation increased rapidly from 32.41 to 208.73 $\text{mL}\cdot\text{min}^{-1}$, indicating the temperature-promoted catalytic activity. Furthermore, according to the values of the rate constant (k) calculated from the slope of the linear part of each plot in Fig. 10a, the activation energy (E_a) of catalytic reaction can be determined. Fig. 10b shows the Arrhenius plot of $\ln k$ vs. the reciprocal absolute temperature ($1/T$). The E_a is estimated to be about 49.27 $\text{kJ}\cdot\text{mol}^{-1}$, which is lower than the reported values for the NaBH_4 hydrolysis catalyzed by hydroxyapatite-supported Co nanoclusters (50 $\text{kJ}\cdot\text{mol}^{-1}$) [38], Co/IR-120 (66.67 $\text{kJ}\cdot\text{mol}^{-1}$) [39], Ru/MMT (54.5 $\text{kJ}\cdot\text{mol}^{-1}$) [40], carbon-supported Co-B (56.72 $\text{kJ}\cdot\text{mol}^{-1}$) [41], attapulgite clay-supported Co-B (56.32 $\text{kJ}\cdot\text{mol}^{-1}$) [42], Co-Cu-B (49.6 $\text{kJ}\cdot\text{mol}^{-1}$) [43], Co-La-Zr-B (53 $\text{kJ}\cdot\text{mol}^{-1}$) [44], Ni-Ru/50WX8 (52.73

kJ mol^{-1}) [45], graphite supported Ru ($61.10 \text{ kJ mol}^{-1}$) [46], and Ru/C ($52.12 \text{ kJ mol}^{-1}$) [47].

Considering that the catalyst's durability is critical to the practical application, we performed recycling experiments to evaluate the reusability of the LSC/Ag_{0.1}Co_{0.9} catalyst. After catalytic reaction, the LSC/Ag_{0.1}Co_{0.9} catalyst can be effectively separated by using an external magnet, due to its sensitively magnetic response (Fig. 1). By combination of the magnetic recyclability, the catalytic activity test was repeated four times, and the results are shown in Fig. 11. It is found that the catalytic activity of the LSC/Ag_{0.1}Co_{0.9} decreases continuously with increasing the cycling time. Similar observations were reported in other bimetallic catalytic systems [14, 48, 49]. The decrease of recycle stability could be attributed to the increased viscosity of the solution and deactivation effect of the increasing metaborate concentration during the hydrolysis process.

4. Conclusions

In summary, we demonstrate that the hydrothermal-derived loofah sponge carbon can be served as an effective solid support for loading bimetallic nanoparticles. The as-fabricated LSC/AgCo exhibited superior performance for the catalytic hydrolysis of NaBH₄ towards hydrogen generation. The LSC can stabilize the AgCo NPs to promote the hydrogen generation efficiency during the catalytic hydrolysis process. The LSC/AgCo catalysts also show the composition-dependent catalytic activity, with LSC/Ag_{0.1}Co_{0.9} being the most active. The catalytic hydrolysis process was found to be affected by other factors, such as substrate concentration and reaction temperature. The activation energy for catalytic hydrolysis reaction is $49.27 \text{ kJ}\cdot\text{mol}^{-1}$. The as-prepared LSC/AgCo catalysts with high hydrogen generation efficiency and low activation energy provides an effective pathway for the economical and sustainable implementation of biomass for the chemical hydrogen storage.

Acknowledgements

This work was supported by the National Natural Science Foundation of China (21103141 and 21207108), the Sichuan Youth Science and Technology Foundation (2013JQ0012), and the Research Foundation of CWNU (12B018).

Appendix A. Supporting information

Supplementary data associated with this article can be found in the online version at <http://dx.doi.org/10.1016/j.jallcom. xxxxxxxx>.

References

- [1] S. Zinoviev, F. Muller-Langer, P. Das, N. Bertero, P. Fornasiero, M. Kaltschmitt, G. Centi, S. Miertus, *ChemSusChem* 3 (2010) 1106-1133.
- [2] M. Li, D.A. Cullen, K. Sasaki, N.S. Marinkovic, K. More, R.R. Adzic, *J. Am. Chem. Soc.* 135 (2013) 132-141.
- [3] L. Chong, J. Zou, X. Zeng, W. Ding, *J. Mater. Chem. A* 1 (2013) 3983-3991.
- [4] M. Yadav, Q. Xu, *Energy Environ. Sci.* 5 (2012) 9698-9725.
- [5] Z. Sun, J. Masa, W. Xia, D. Konig, A. Ludwig, Z.-A. Li, M. Farle, W. Schuhmann, M. Muhler, *ACS Catal.* 2 (2012) 1647-1653.
- [6] M. Heggen, M. Oezaslan, L. Houben, P. Strasser, *J. Phys. Chem. C* 116 (2012) 19073-19083.
- [7] H. Yin, S. Liu, C. Zhang, J. Bao, Y. Zheng, M. Han, Z. Dai, *ACS Appl. Mater. Interfaces* 6 (2014) 2086-2094.
- [8] D. Sun, V. Mazumder, O. Metin, S. Sun, *ACS Catal.* 2 (2012) 1290-1295.
- [9] D. Sun, V. Mazumder, O. Metin, S. Sun, *ACS Nano* 5 (2011) 6458-6464.

- [10] J.-M. Yan, X.-B. Zhang, T. Akita, M. Haruta, Q. Xu, *J. Am. Chem. Soc.* 132 (2010) 5326-5327.
- [11] H.-L. Jiang, T. Akita, Q. Xu, *Chem. Commun.* 47 (2011) 10999-11001.
- [12] N. Cao, J. Su, W. Luo, G. Cheng, *Int. J. Hydrogen Energy* 39 (2014) 426-435.
- [13] L. Yang, J. Su, W. Luo, G. Cheng, *Int. J. Hydrogen Energy* 39 (2014) 3360-3370.
- [14] W. Feng, L. Yang, N. Cao, C. Du, H. Dai, W. Luo, G. Cheng, *Int. J. Hydrogen Energy* 39 (2014) 3371-3380.
- [15] L. Yang, J. Su, X. Meng, W. Luo, G. Cheng, *J. Mater. Chem. A* 1 (2013) 10016-10023.
- [16] X. Gu, Z.-H. Lu, H.-L. Jiang, T. Akita, Q. Xu, *J. Am. Chem. Soc.* 133 (2011) 11822-11825.
- [17] H.-L. Jiang, T. Akita, T. Ishida, M. Haruta, Q. Xu, *J. Am. Chem. Soc.* 133 (2011) 1304-1306.
- [18] J. Li, Q.-L. Zhu, Q. Xu, *Chem. Commun.* 50 (2014) 5899-5901.
- [19] P.-Z. Li, K. Aranishi, Q. Xu, *Chem. Commun.* 48 (2012) 3173-3175.
- [20] L. Ai, H. Yue, J. Jiang, *J. Mater. Chem.* 22 (2012) 23447-23453.
- [21] L. Ai, J. Jiang, *Bioresour. Technol.* 132 (2013) 374-377.
- [22] L. Ai, X. Gao, J. Jiang, *J. Power Sources* 257 (2014) 213-220.
- [23] N.S. Sobal, M. Hilgendorff, H. Mohwald, M. Giersig, *Nano Lett.* 2 (2002) 621-624.
- [24] L. Yang, W. Luo, G. Cheng, *ACS Appl. Mater. Interfaces* 5 (2013) 8231-8240.
- [25] P. Nowicki, R. Pietrzak, H. Wachowska, *Energy Fuels* 24 (2010) 1197-1206.
- [26] V.O.A. Tanobe, T.H.D. Sydenstricker, M. Munaro, S.C. Amico, *Polym. Testing* 24 (2005) 474-482.
- [27] Q. Jiao, M. Fu, C. You, Y. Zhao, H. Li, *Inorg. Chem.* 51 (2012) 11513-11520.

- [28] M. Pang, J. Hu, H.C. Zeng, *J. Am. Chem. Soc.* 132 (2010) 10771-10785.
- [29] G.M. Arzac, T.C. Rojas, A. Fernández, *Appl. Catal. B* 128 (2012) 39-47.
- [30] T.A. Maark, A.A. Peterson, *J. Phys. Chem. C* 118 (2014) 4275-4281.
- [31] A.E. Baber, H.L. Tierney, E.C.H. Sykes, *ACS Nano* 4 (2010) 1637-1645.
- [32] J.B. Henry, A. Maljusch, M. Huang, W. Schuhmann, A.S. Bondarenko, *ACS Catal.* 2 (2012) 1457-1460.
- [33] B. Zhou, M. Wen, Q. Wu, *Nanoscale* 5 (2013) 8602-8608.
- [34] J. Gu, Y.W. Zhang, F. Tao, *Chem. Soc. Rev.* 41 (2012) 8050-8065.
- [35] F. Li, Q. Li, H. Kim, *Chem. Eng. J.* 210 (2012) 316-324.
- [36] M. Zahmakiran, S. Ozkar, *Langmuir* 25 (2009) 2667-2678.
- [37] N. Sahiner, O. Ozay, E. Inger, N. Aktas, *Appl. Catal. B: Environ.* 102 (2011) 201-206.
- [38] M. Rakap, S. Özkar, *Catal. Today* 183 (2012) 17-25.
- [39] C.-H. Liu, B.-H. Chen, C.-L. Hsueh, J.-R. Ku, F. Tsau, K.-J. Hwang, *Appl. Catal. B: Environ.* 91 (2009) 368-379.
- [40] S. Peng, X. Fan, J. Zhang, F. Wang, *Appl. Catal. B: Environ.* 140-141 (2013) 115-124.
- [41] F. Baydaroglu, E. Ozdemir, A. Hasimoglu, *Int. J. Hydrogen Energy* 39 (2014) 1516-1522.
- [42] H. Tian, Q. Guo, D. Xu, *J. Power Sources* 195 (2010) 2136-2142.
- [43] X.-L. Ding, X. Yuan, C. Jia, Z.-F. Ma, *Int. J. Hydrogen Energy* 35 (2010) 11077-11084.
- [44] M.H. Loghmani, A.F. Shojaei, *Int. J. Hydrogen Energy* 38 (2013) 10470-10478.
- [45] C.-H. Liu, B.-H. Chen, C.-L. Hsueh, J.-R. Ku, M.-S. Jeng, F. Tsau, *Int. J. Hydrogen Energy* 34 (2009) 2153-2163.
- [46] Y. Liang, H.-B. Dai, L.-P. Ma, P. Wang, H.-M. Chen, *Int. J. Hydrogen Energy* 35 (2010)

3023-3028.

[47] Y.C. Zou, M. Nie, Y.M. Huang, J.Q. Wang, H.L. Liu, Int. J. Hydrogen Energy 36 (2011)

12343-12351.

[48] D.-R. Kim, K.-W. Cho, Y.-I. Choi, C.-J. Park, Int. J. Hydrogen Energy 34 (2009)

2622-2630.

[49] C. Du, J. Su, W. Luo, G. Cheng, J. Mol. Catal. A 383-384 (2014) 38-45.

ACCEPTED MANUSCRIPT

Figure captions

Fig. 1. Schematic illustration for the synthesis procedure of LSC/AgCo catalyst

Fig. 2. FTIR spectrum of the LSC

Fig. 3. XRD patterns of the LSC, free $\text{Ag}_{0.1}\text{Co}_{0.9}$ and LSC/ $\text{Ag}_{0.1}\text{Co}_{0.9}$

Fig. 4. SEM images of the LSC (a,b), free $\text{Ag}_{0.1}\text{Co}_{0.9}$ (c,d) and LSC/ $\text{Ag}_{0.1}\text{Co}_{0.9}$ (e,f)

Fig. 5. XPS spectra of the LSC/ $\text{Ag}_{0.1}\text{Co}_{0.9}$: (a) C 1s, (b) O 1s, (c) Co 2p and (d) Ag 3d

Fig. 6. Hydrogen generation from NaBH_4 aqueous solution (5 wt%) catalyzed by LSC, free $\text{Ag}_{0.1}\text{Co}_{0.9}$ and LSC/ $\text{Ag}_{0.1}\text{Co}_{0.9}$ at 30 °C

Fig. 7. (a) Hydrogen generation from NaBH_4 aqueous solution (5 wt%) catalyzed by LSC/ $\text{Ag}_x\text{Co}_{1-x}$ ($x = 0, 0.1, 0.2, 0.3, 0.5,$ and 1) at 30 °C. (b) Activity enhancement factor ($k_{\text{LSC}/\text{AgCo}}/k_{\text{LSC}/\text{Co}}$) and the corresponding apparent reaction rate k (inset) of LSC/ $\text{Ag}_x\text{Co}_{1-x}$

Fig. 8. Catalytic activity of the LSC/ $\text{Ag}_{0.1}\text{Co}_{0.9}$ toward the hydrogen generation by hydrolysis of NaBH_4 solution (5 wt%) containing different concentrations of NaOH at 30 °C

Fig. 9. Catalytic activity of the LSC/ $\text{Ag}_{0.1}\text{Co}_{0.9}$ toward the hydrogen generation by hydrolysis of different concentrations of NaBH_4 solution containing 5 wt% NaOH at 30 °C

Fig. 10. (a) Catalytic activity of the LSC/ $\text{Ag}_{0.1}\text{Co}_{0.9}$ toward the hydrogen generation by hydrolysis of NaBH_4 solution (5 wt%) containing 5 wt% NaOH at different temperatures. (b) Arrhenius plot of $\ln k$ vs. the reciprocal absolute temperature ($1/T$)

Fig. 11. Reusability test of hydrogen generation from hydrolysis of NaBH_4 solution (5 wt%) containing 5 wt% NaOH catalyzed by the LSC/ $\text{Ag}_{0.1}\text{Co}_{0.9}$ at 30 °C

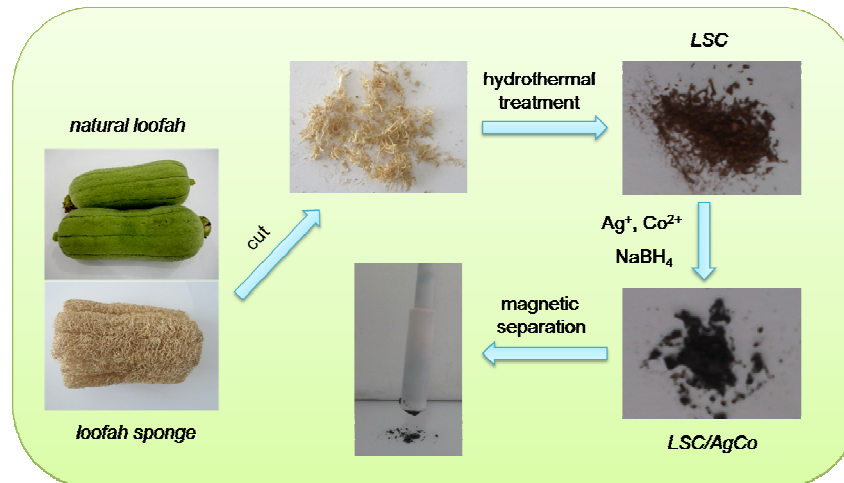


Fig. 1.

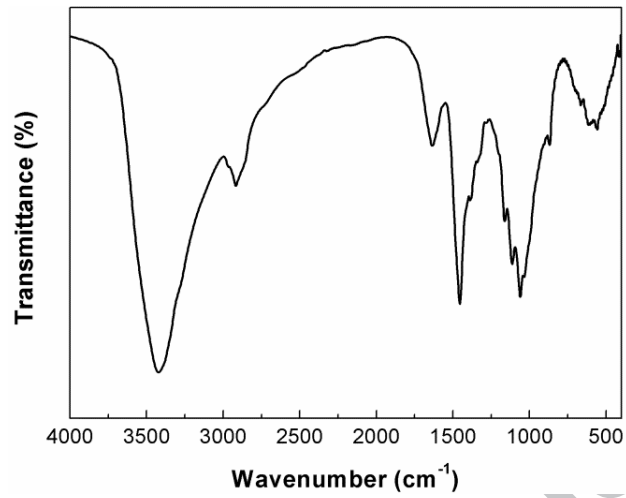


Fig. 2.

ACCEPTED MANUSCRIPT

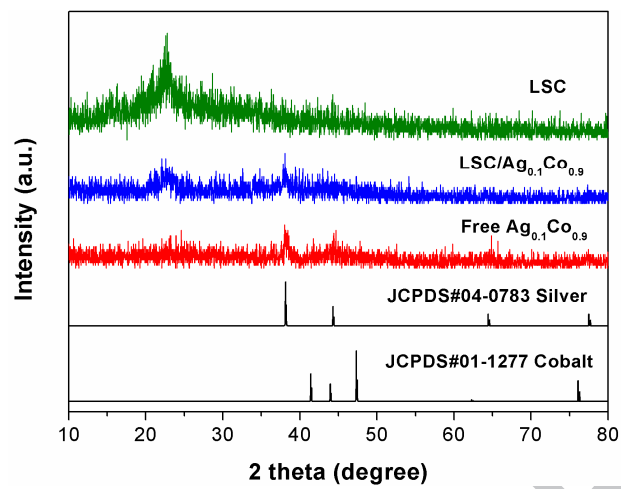


Fig. 3.

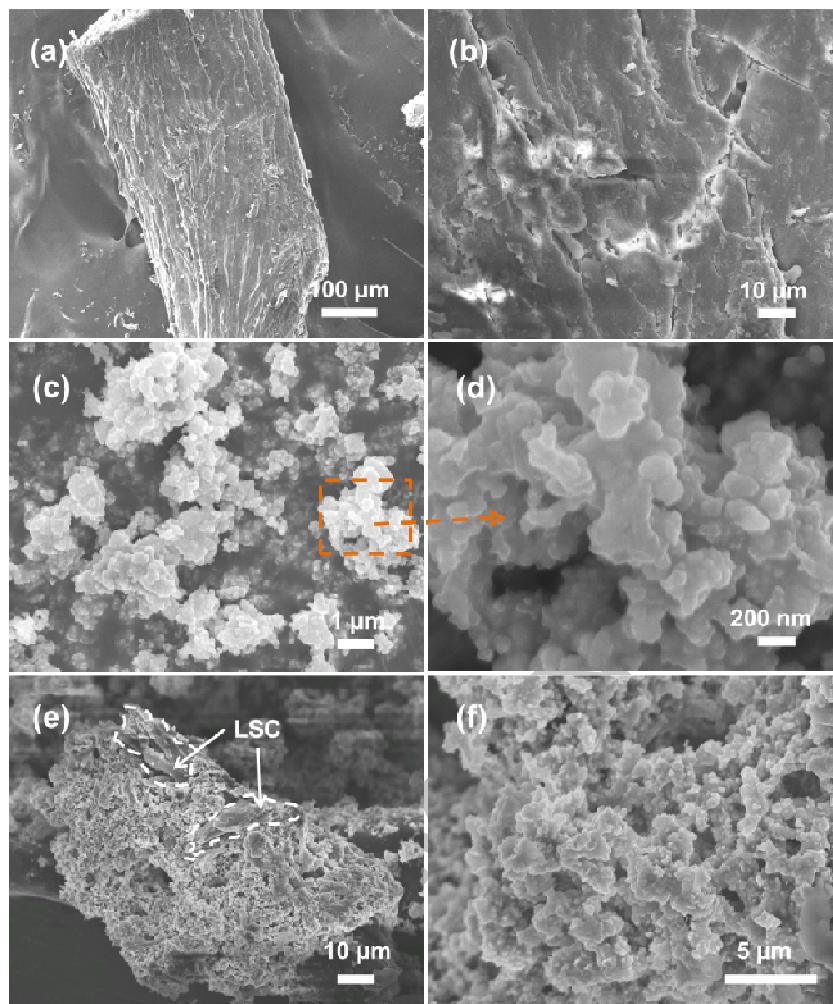


Fig. 4.

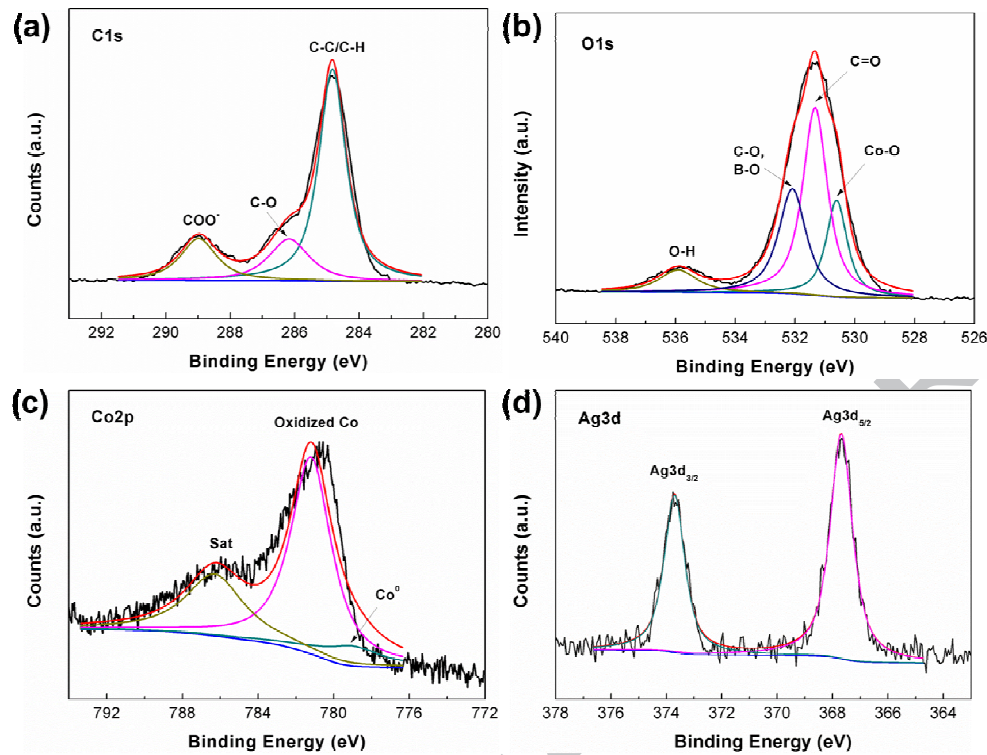


Fig. 5.

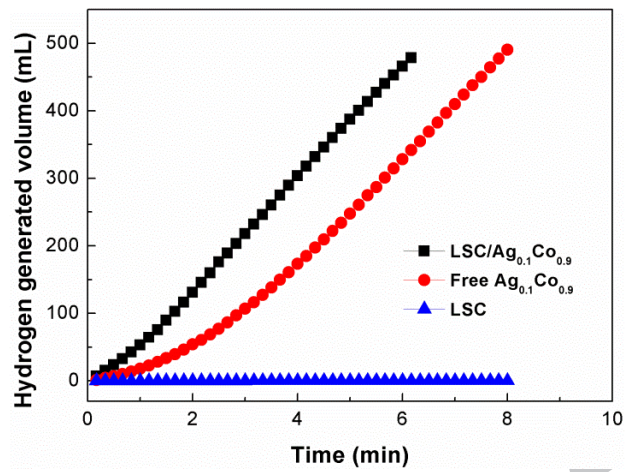


Fig. 6.

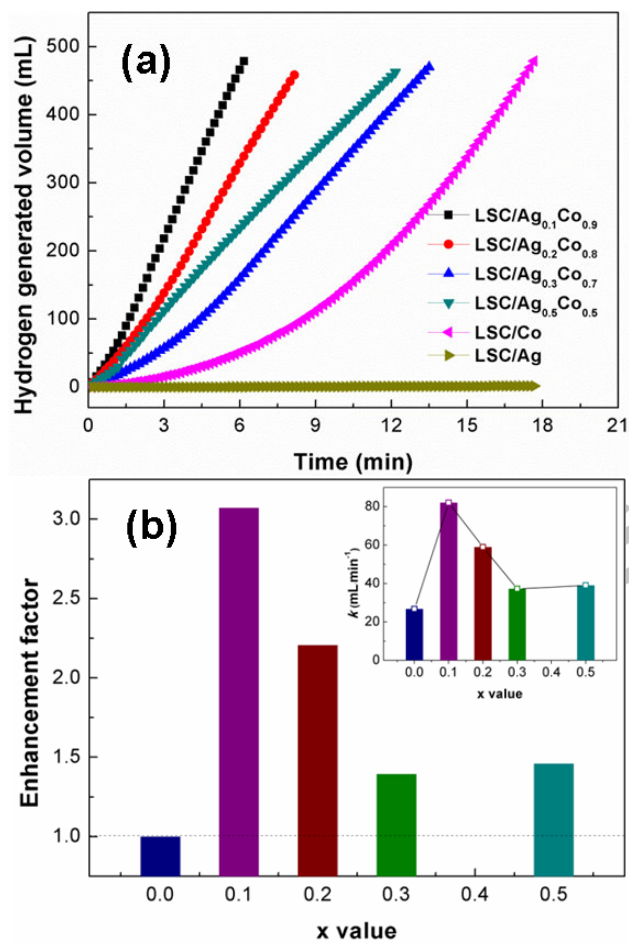


Fig. 7.

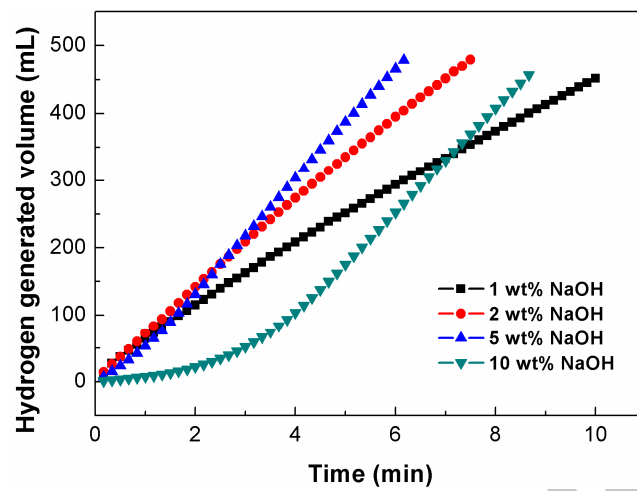


Fig. 8.

ACCEPTED MANUSCRIPT

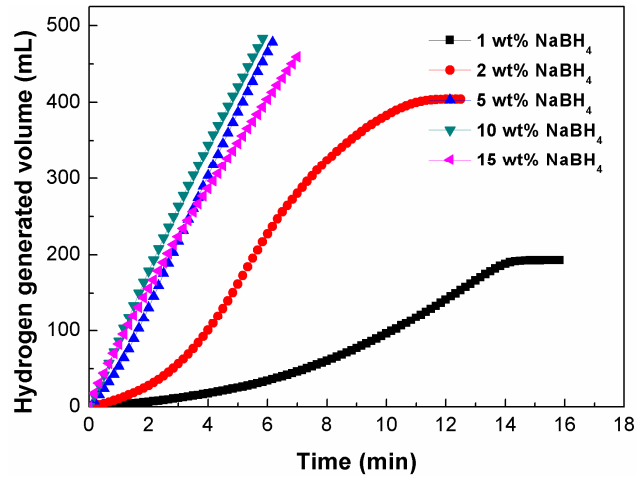


Fig. 9.

ACCEPTED MANUSCRIPT

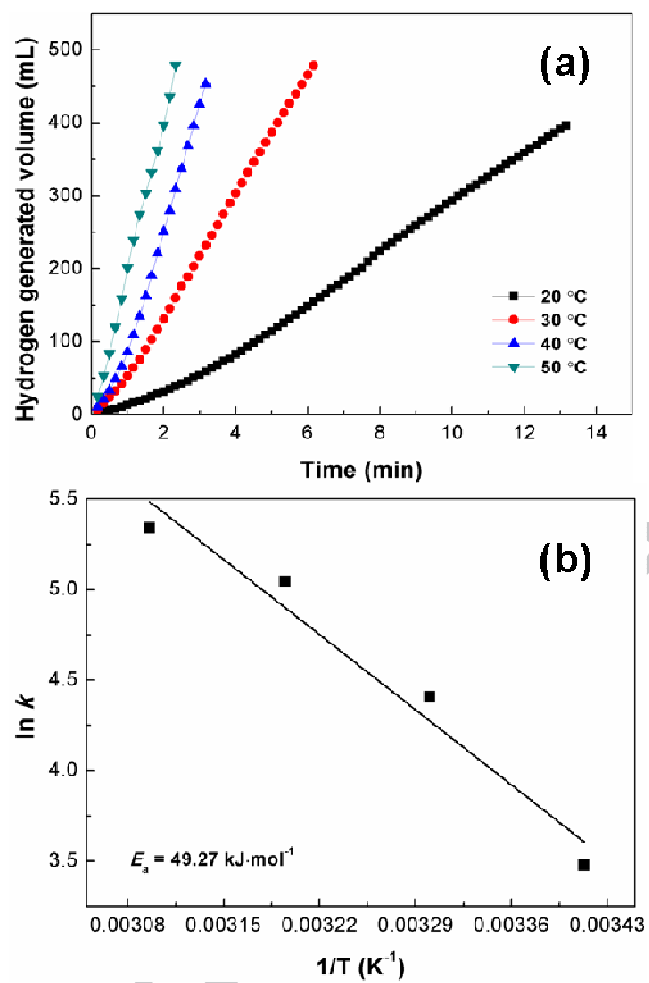


Fig. 10.

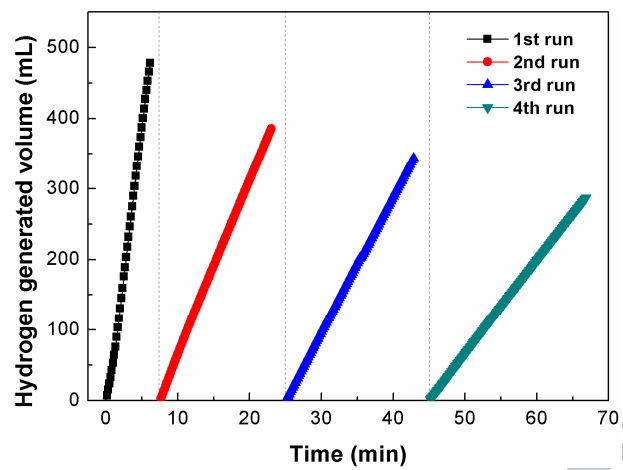


Fig. 11.

ACCEPTED MANUSCRIPT

□ Bimetallic AgCo nanoparticles supported on loofah sponge carbon is synthesized.

□ The LSC/AgCo catalyst exhibits high performance in the hydrolysis of NaBH₄.

□ LSC/Ag_{0.1}Co_{0.9} is most active among all of the catalysts.

□ Supporting effect and alloying effect in LSC/AgCo catalysts cooperate together to efficiently catalyze NaBH₄ hydrolysis.

ACCEPTED MANUSCRIPT